



Chemical interference with DSIF complex formation lowers synthesis of mutant huntingtin gene products and curtails mutant phenotypes

Ning Deng^{a,1} , Yun-Yun Wu^{b,c,1}, Yanan Feng^a, Wen-Chieh Hsieh^c, Jen-Shin Song^d, Yu-Shiuan Lin^c, Ya-Hsien Tseng^c, Wan-Jhu Liao^c, Yi-Fan Chu^e, Yu-Cheng Liu^f , En-Cheng Chang^c , Chia-Rung Liu^f, Sheh-Yi Sheu^g , Ming-Tsan Su^g, Hung-Chih Kuo^h, Stanley N. Cohen^{a,2} , and Tzu-Hao Cheng^{b,c,i,2}

Edited by Nancy Bonini, University of Pennsylvania, Philadelphia, PA; received March 17, 2022; accepted June 30, 2022

Earlier work has shown that siRNA-mediated reduction of the SUPT4H or SUPT5H proteins, which interact to form the DSIF complex and facilitate transcript elongation by RNA polymerase II (RNAPII), can decrease expression of mutant gene alleles containing nucleotide repeat expansions differentially. Using luminescence and fluorescence assays, we identified chemical compounds that interfere with the SUPT4H-SUPT5H interaction and then investigated their effects on synthesis of mRNA and protein encoded by mutant alleles containing repeat expansions in the huntingtin gene (*HTT*), which causes the inherited neurodegenerative disorder, Huntington's Disease (HD). Here we report that such chemical interference can differentially affect expression of *HTT* mutant alleles, and that a prototypical chemical, 6-azauridine (6-AZA), that targets the SUPT4H-SUPT5H interaction can modify the biological response to mutant *HTT* gene expression. Selective and dose-dependent effects of 6-AZA on expression of *HTT* alleles containing nucleotide repeat expansions were seen in multiple types of cells cultured in vitro, and in a *Drosophila melanogaster* animal model for HD. Lowering of mutant HD protein and mitigation of the *Drosophila* "rough eye" phenotype associated with degeneration of photoreceptor neurons in vivo were observed. Our findings indicate that chemical interference with DSIF complex formation can decrease biochemical and phenotypic effects of nucleotide repeat expansions.

SUPT4H | Spt4 | Huntington's disease | DSIF | nucleotide repeats

Expansion of the number of contiguous nucleotide repeats that normally exist within certain human genes is the cause of multiple human diseases (1–3). Earlier work has shown that expression of alleles containing nucleotide repeat expansions can be reduced differentially by inhibiting production of SUPT4H or SUPT5H, highly conserved cellular proteins that interact to form the transcription elongation complex, DSIF (5,6-dichloro-1-β-d-ribofuranosylbenzimidazole sensitivity-inducing factor) (4, 5). DSIF assists in the elongation of mRNA molecules by attaching to RNA polymerase II (RNAPII) via an SUPT5H binding site and forming a structural clamp that maintains RNAPII occupancy of template DNA as the polymerase proceeds along the template (6–8). A decrease in production or function of SUPT4H or SUPT5H has been found to decrease synthesis of transcripts encoded by genes containing nucleotide repeat expansions (9–14) including *HTT*, the gene that causes Huntington's Disease (for recent reviews see (15–17)), the *C9orf72* locus associated with amyotrophic lateral sclerosis and frontotemporal dementia (for review see (18)), and *NOP56*, the gene associated with spinocerebellar atrophy type 36 (SCA36) (19), and it has been suggested that SUPT4H or SUPT5H may be a target for treatment of certain diseases caused by nucleotide repeat expansions (9–14, 20). As interaction between SUPT4H and SUPT5H to form the DSIF complex is required for these proteins to form the structural clamp that maintains RNAPII on DNA template (8), we sought to identify compounds that interfere with the SUPT4H-SUPT5H interaction and to elucidate their effects on mutant *HTT* gene products. Here we describe the results of experiments aimed at: 1) identifying chemicals that can interfere with the SUPT4H/5H interaction, 2) determining whether chemical interference with the interaction recapitulates the effects of decreasing SUPT4H or SUPT5H on expression of genes containing expanded nucleotide repeats, and 3) determining whether chemical interference with the interaction has phenotypic effects.

Results

Chemical Interference with Interaction of SUPT4H and SUPT5H-NGN. We developed and used two high-throughput screening assays in parallel in human cells to identify

Significance

Multiple inherited diseases are caused by expansion in the number of contiguous nucleotide repeats in certain human genes. Normal progression of RNA polymerase II along DNA templates is aided by the DSIF complex formed by interaction of the SUPT4H and SUPT5H proteins. This report shows that chemical interference with DSIF formation can selectively reduce expression of gene alleles containing expanded repeats and further identifies a prototypical DSIF-disrupting chemical that can mitigate disease-related phenotypes associated with repeat expansion.

Author contributions: N.D., Y.Y.W., Y.F., W.C.H., C.R.L., S.N.C., and T.H.C. designed research; N.D., Y.Y.W., Y.F., J.S.S., Y.S.L., Y.H.T., W.J.L., Y.F.C., Y.C.L., and E.C.C. performed research; N.D., Y.F., J.S.S., S.Y.S., M.T.S., and H.C.K. contributed new reagents/analytic tools; N.D., Y.Y.W., Y.F., J.S.S., Y.S.L., Y.H.T., W.J.L., Y.F.C., Y.C.L., S.N.C., and T.H.C. analyzed data; and N.D., Y.Y.W., S.N.C., and T.H.C. wrote the paper.

The authors declare no competing interest.

This article is a PNAS Direct Submission.

Copyright © 2022 the Author(s). Published by PNAS. This article is distributed under [Creative Commons Attribution-NonCommercial-NoDerivatives License 4.0 \(CC BY-NC-ND\)](https://creativecommons.org/licenses/by-nc-nd/4.0/).

¹N.D. and Y.Y.W. contributed equally to this work.

²To whom correspondence may be addressed. Email: sncohen@stanford.edu or thcheng@nycu.edu.tw.

This article contains supporting information online at <http://www.pnas.org/lookup/suppl/doi:10.1073/pnas.2204779119/-/DCSupplemental>.

Published August 1, 2022.

events that interfere with luminescence or fluorescence signals which result from interaction between reporter gene tags attached to SUPT4H and SUPT5H. A protein-fragment complementation assay (PCA) quantified luminescence resulting from interaction between *Gussia* luciferase (Gluc) subunit fragments (GL1 and GL2) (21) fused separately to SUPT4H or to the NGN domain of SUPT5H (Fig. 1A). A bimolecular fluorescence complementation (BiFC) assay (22) used analogous fluorescence-generating tags (*SI Appendix*, Fig. S1) to detect interaction between SUPT4H and SUPT5H-NGN. Expression of fusion proteins in both assays was under control of inducible promoters (Fig. 1B and C, and *SI Appendix*, Fig. S1A and B).

A library comprised of ~140,000 compounds having diverse chemical structures was screened in a human HEK 293 cell line, M2-8, that we engineered to express SUPT4H-GL1 and SUPT5H-NGN-GL2 fusion proteins encoded by chromosomally inserted genes. The steps in the screening procedures are diagrammed in Fig. 1D and *SI Appendix*, Fig. S1C. A cell line

(i.e., G5; Fig. 1D) which expresses intact Gluc protein and consequently emits a luminescence signal that is independent of interaction between SUPT4H and SUPT5H-NGN was used as a negative control for compound effect. A separate library of 60,000 low-molecular weight chemicals was screened in HeLa cells using the BiFC assay. Compounds that produced a signal in one assay were tested in the other, and only chemicals that affected both assays were investigated further.

Among the compounds identified in our screens were multiple nucleosides that included 6-azauridine (6-AZA), a known global inhibitor of nucleic acid synthesis, and its triacetylated derivative, 6-AZA-TA (23) (Fig. 2A, and *SI Appendix*, Fig. S2). In contrast to these compounds, ribavirin, a closely related nucleoside inhibitor of nucleic acid synthesis, showed no detectable signal (Fig. 2A). We noted that 6-AZA is the riboside of 6-azauracil (6AU), which previously was reported to have its actions in yeast cells affected by mutations that alter the interaction of RNAPII with Spt5, the *S. cerevisiae* ortholog

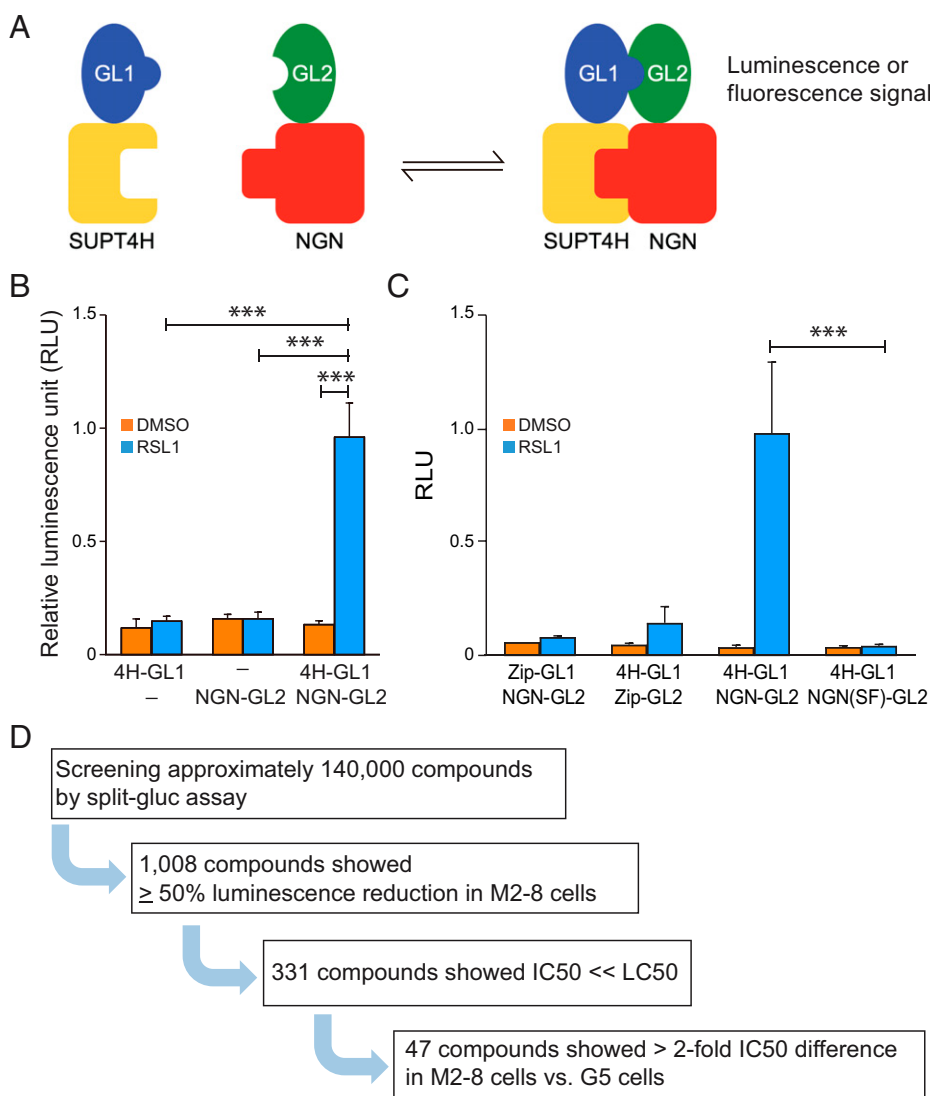


Fig. 1. Interaction between SUPT4H and NGN domain of SUPT5H. (A) Schematic diagram depicting the interaction between SUPT4H and NGN to yield a luminescence signal by bringing together fragments of the split-*Gussia* luciferase (Gluc). (B) Bar graph showing relative luminescence generated by the indicated constructs in the presence of the expression-inducing ligand RSL1 (RheoSwitch ligand 1) or a noninducing control element (DMSO). (C) Relative luminescence units (RLU) generated by cotransfection mediated complementation between Gluc reporter fragments fused to SUPT4H (4H-GL1). Controls were fusion proteins containing a leucine zipper motif capable of forming homodimers but not able to interact with SUPT4H or NGN (Zip-GL1 and Zip-GL2), or NGN (NGN-GL2). The NGN(SF)-GL2 construct contains a 214 Ser-to-Phe substitution in NGN known to preclude NGN interaction with SUPT4H. The values shown in panels B and C are the mean \pm SD ($n = 4$; $***P < 0.001$, two-tailed paired Student's t test). (D) Screening procedures for identification of small molecules that interfere with the luminescence segment generated by interaction between SUPT4H and SUPT5H-NGN. Z'-factor = 0.83.

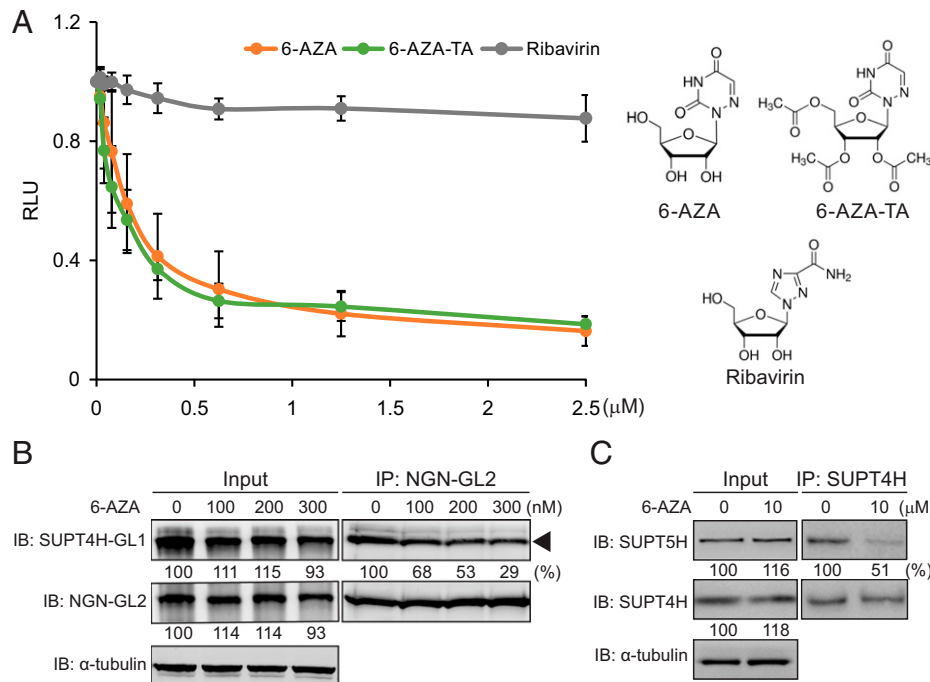


Fig. 2. Effect of 6-azauridine (6-AZA) and 6-AZA-TA. (A) Comparison of 6-AZA and related compounds on luminescence generated by the SUPT4H-SUPT5H-NGN interaction. M2-8 cells were incubated with compounds having chemical structures as shown, and luminescence signals determined for each sample were quantified using procedures described in Materials and Methods. The signal from lysates of untreated cells (i.e., relative luminescence units; RLU) was set as 1. Mean values \pm SDs are indicated. ($n = 3$) (B) Western blot of immunoprecipitation analysis of SUPT4H interaction with SUPT5H-NGN. M2-8 cells were treated with 6-AZA at indicated concentrations. Flag-tagged NGN-GL2 protein was collected by immunoprecipitation using anti-Flag magnetic beads. The precipitates were then probed and quantitated using anti-Gluc antibody as indicated in Materials and Methods to detect SUPT4H-GL1 (arrowhead) that had coprecipitated with NGN-GL2. Band intensity measurements determined for SUPT4H-GL1 were normalized against NGN-GL2 measurements and the intensity of the SUPT4H-GL1 band relative to NGN-GL2 is indicated by %. The normalized value for the untreated sample was set as 100%. (C) Analysis of endogenous SUPT4H interaction with SUPT5H. ST Hdh^{Q111/Q111} cells were treated with 10 μ M 6-AZA for 24 h. Protein lysates were collected and subjected to immunoprecipitation using anti-SUPT4H antibody. Precipitates were then probed by anti-SUPT4H and anti-SUPT5H antibody respectively. SUPT5H band intensity was measured and normalized to that of SUPT4H. The normalized value for the untreated sample was set as 100%. ($n = 3$).

of SUPT5H (24), prompting our further interest in 6-AZA. The ability of 6-AZA to reduce abundance of the SUPT4H-SUPT5H-NGN or cellular SUPT4H-SUPT5H complex, as observed in both our luminescence-based reporter gene assay and murine neuronal cells, was confirmed biochemically by immunoprecipitation analysis (Fig. 2 B and C).

Effects of 6-AZA on Expression of Mutant HTT Protein. We investigated the effects of 6-AZA on the cellular production of mRNA and protein encoded by mutant and normal *HTT* alleles. Three different cell contexts containing repeat expansions of different lengths were investigated: immortalized lymphoblastoid cells derived from peripheral blood of an HD patient, immortalized murine striatal neurons containing a mutant human *HTT* allele, and nonproliferating neurons generated in culture from stem cells derived from HD patient fibroblasts. We found that 6-AZA affected mutant HTT expression in all three cell types and that the magnitude and specificity of effects differed in the different cell contexts.

In the human lymphoblastoid cell line (GM14044), which harbors a mutant *HTT* allele containing 750 repeats of CAG (25–27), Western blot analysis indicated that treatment with nanomolar concentrations of 6-AZA reduced mutant HTT to half its original abundance, relative to total protein, while resulting in no diminution of protein encoded by the normal *HTT* allele (Fig. 3A, left and right panels). Differential effects of 6-AZA on mutant versus wild type *HTT* gene products were also observed in cultured striatal neurons derived from mice that had been engineered to contain 111 CAG repeats in both *HTT* alleles (ST Hdh^{Q111/Q111}) (28) (Fig. 3B and SI Appendix,

Fig. S3A). In these cells the effects of 6-AZA treatment on mutant HTT mRNA and protein abundance were observed only at or above micromolar concentrations of the compound, which also reduced cell viability, as assessed by cell number (Fig. 3C). Addition of uridine to cell cultures reversed the inhibitory effect of 6-AZA on the synthesis of DNA and RNA and was accompanied by a dose-dependent increase of cell number and reversal of 6-AZA-mediated loss of cell viability (Fig. 3D and SI Appendix, Figs. S4 A and B)—consistent with the known effects of 6-AZA-induced uridine-5'-monophosphate depletion. In contrast, uridine addition did not detectably affect the lowering of mutant HTT by 6-AZA (Fig. 3E), nor alter the inhibitory effect of 6-AZA on DSIF complex formation (SI Appendix, Fig. S4C), demonstrating that these latter effects are not a consequence of uridine insufficiency.

The third cell context tested consisted of human neural cells that we generated in vitro from stem cells. Neurons present in the *corpus striatum* region of the brain are mostly medium-sized cells that have spiny projections and express gamma-aminobutyric acid (GABA) on their surface; such cells have been called medium spiny neurons (MSNs) (29). Like MSNs present in the brain, MSNs generated in vitro from progenitor cells do not undergo cell division (30). The MSNs used in our experiments (i.e., MSN-GM23225 cells) were derived from stem cells obtained by de-differentiation of cutaneous fibroblasts from an HD patient bearing 72 CAG repeats in the mutant *HTT* allele (SI Appendix, Fig. S5 A and B) (31). As seen in Fig. 3F and SI Appendix, Fig. S3B, 6-AZA-mediated lowering of mutant HTT protein and mRNA in MSN-GM23225 cells also required micromolar concentrations of 6-AZA. In MSN cells, mutant HTT protein was

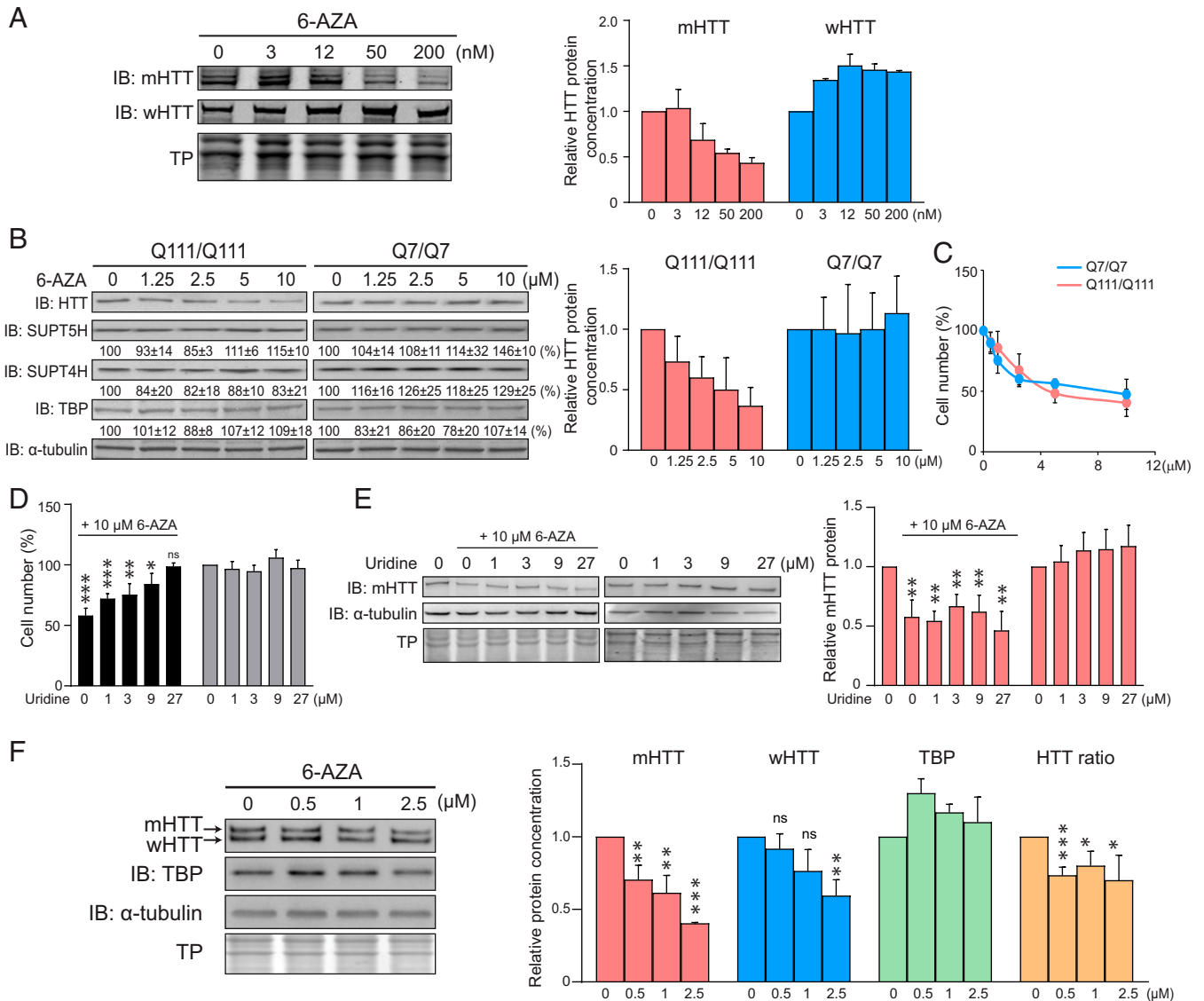


Fig. 3. Effects of 6-AZA on protein production by mutant or normal *HTT* alleles. (A) Effects in GM14044 human lymphoblastoid cells, a mutant *HTT* allele containing 750 CAG repeats and a normal allele containing 19 CAG repeat cells, treated with indicated concentrations of 6-AZA were subjected to Western blot analysis (left). Relative protein abundance was calibrated by scanning and normalized against total protein (TP) and the normalized values were plotted (right). Proteins in untreated samples were set as 1. (B) HTT, SUPT5H, SUPT4H, and TBP proteins in *ST Hdh*^{Q111/Q111} and *ST Hdh*^{Q7/Q7} cells treated with 6-AZA were detected by Western blotting (left). Values were normalized against α -tubulin and plotted (right). The value obtained for each protein from untreated sample was set as 1. (C) Measurement of cell number in cells treated with Q7/Q7 and Q111/Q111 with 6-AZA concentrations shown in B. (D) Effect of the indicated concentrations of uridine on relative number of *ST Hdh*^{Q111/Q111} cells incubated with 10 μ M 6-AZA (left) or lacking 6-AZA (right) are shown. The viability of cells grown in the absence of either agent was set to 100%. (E) *ST Hdh*^{Q111/Q111} cells treated with 10 μ M 6-AZA as described in D were analyzed by Western blotting and values were normalized against those obtained for total protein (TP). Samples collected from 6-AZA treated cells were shown a line above the panel. Quantification of the effects on mHTT protein in 6-AZA treated vs. untreated cells shown at the right panel. The relative occurrence of mHTT protein value in cells not exposed to either 6-AZA or uridine was set as 1. Mean values and \pm SDs are indicated. (F) Effects of 6-AZA on MSN-GM23225 cells. Protein lysates were collected and analyzed by Western blotting (left) for the abundance of mHTT, wHTT, TBP, and α -tubulin relative to total protein (TP) and compared to the value obtained for cells lacking 6-AZA treatment, which was set to 1 (right). HTT ratio represents the calculated value of mHTT vs. wHTT. Error bars represent the SD. ($n = 3$; ns: no significant, $*P < 0.05$, $**P < 0.01$, $***P < 0.001$, two-tailed paired Student's *t* test).

decreased to half the original abundance (Fig. 3F) at a compound concentration of 2.5 μ M. At this 6-AZA concentration, HTT protein encoded by the wild type *HTT* allele, which contained 17 repeats, was also reduced in abundance relative to total protein and to an α -tubulin internal control. Additionally, whereas diminished expression of mutant *HTT* alleles was observed in the immortalized *ST Hdh*^{Q111/Q111} murine cell line after only one day of exposure, in nonproliferating MSN-GM23225 cells 6-AZA effects required at least nine days of exposure—and were most evident after 13 d.

Effect of 6-AZA on Response of HD Cells to Oxidative Stress.
The survival and growth of cells requires neutralization of

reactive oxygen species and other DNA-damaging molecules generated intracellularly during normal metabolism (32). An excess of oxidants relative to antioxidants normally leads to increased production of glutathione-S-transferases (GSTs)—evolutionarily conserved enzymes that neutralize oxidants by conjugating them to reduced glutathione (33). When GSTs are insufficient to cope with an oxidant/antioxidant imbalance, the result is cell dysfunction and loss of viability (i.e., “oxidative stress”) (34).

Neurodegenerative diseases commonly are associated with abnormal mitochondrial function [for recent reviews, see (35–37)], and sensitivity to oxidative stress is increased in cells of persons afflicted with these diseases (38). Steady state expression of GST enzymes is also diminished in cells of HD patients (38–42). To

evaluate the effects of 6-AZA on mutant HTT-associated GST reproduction, we used CRISPR technology to reduce the number of CAG repeats in the mutant *HTT* allele of MSN-GM23225 cells from 72 to 17 (*SI Appendix*, Fig. S6) yielding the congenic cell lines GMC#1 and GMC#2. We observed that such reduction elevated the steady state expression of *GSTT1* and *GSTT2*—two GSTs reported previously to be affected by HD mutations (40, 41) (Fig. 4A).

Consistent with earlier evidence that neurons derived from persons afflicted with HD have increased sensitivity to agents that induce oxidative stress (38), we observed that cell viability upon exposure to H_2O_2 was lower in GM23225 cells than in the congenic lines in which the CAG repeat length had been shortened to a wild type length (Fig. 4B). Exposure to 6-AZA partially reversed the hypersensitivity of GM23225 cells to H_2O_2 , leading to increased cell survival, whereas the compound did not affect H_2O_2 sensitivity of GMC#1 or GMC#2 cells cultured under the same conditions (Fig. 4B). Similarly, the diminished baseline expression of *GSTT1* and *GSTT2* observed in GM23225 cells was reversed by exposure of cells to 6-AZA (Fig. 4A). Collectively, these results suggest that 6-AZA can decrease the effects of *HTT* gene repeat expansions on the cellular response to oxidant exposure.

Effects of 6-AZA on Phenotypic Expression of Mutant Human *HTT* Gene in *Drosophila*. Earlier work has shown that expression in transgenic *Drosophila melanogaster* of human *HTT* inserts containing long CAG repeats results in severe degeneration of photoreceptor neurons in the animals' compound eyes and a phenotypic trait described as 'rough eye' (Fig. 5A); such

photoreceptor neuron degeneration is believed to be analogous to the loss of neurons in the brains of HD patients (43). Transgenic flies containing *HTT* genes having short nucleotide repeats do not show this phenotype (44, 45). Expression of mutant human *HTT* in *Drosophila melanogaster* has been used extensively to assess effects of therapeutic agents on manifestations of HD (46).

Our experiments tested the effect of 6-AZA added to media during larval development on the rough eye phenotype in transgenic flies that express human mutant *HTT* or controls, (*SI Appendix*, Fig. S7). As seen in Fig. 5, the incidence of the rough eye phenotype ranged from 50% to 70% under the experimental conditions we used. This incidence was reduced by almost half (i.e., to 30–40%) by inclusion in agar of 6-AZA or 6-AZA-TA (Fig. 5A). Reduction of the rough eye phenotype by 6-AZA occurred at compound concentrations that did not affect larval viability (Fig. 5B), and immunoblot analysis showed that phenotypic rescue in treated animals was associated with a decrease in mutant *HTT* expression (Fig. 5C).

Discussion

Decreasing the expression of the SUPT4H or SUPT5H components of the DSIF complex can lower production of mRNAs encoded by mutant gene alleles containing nucleotide repeat expansions, and also can modify phenotypes associated with repeat expansions (9, 10, 13, 14). These findings have led to proposals that that chemical or genetic targeting of SUPT4H or SUPT5H may be useful therapeutically (10–14). The results reported here indicate that chemical interference with the interaction of SUPT4H and SUPT5H is achievable, that such

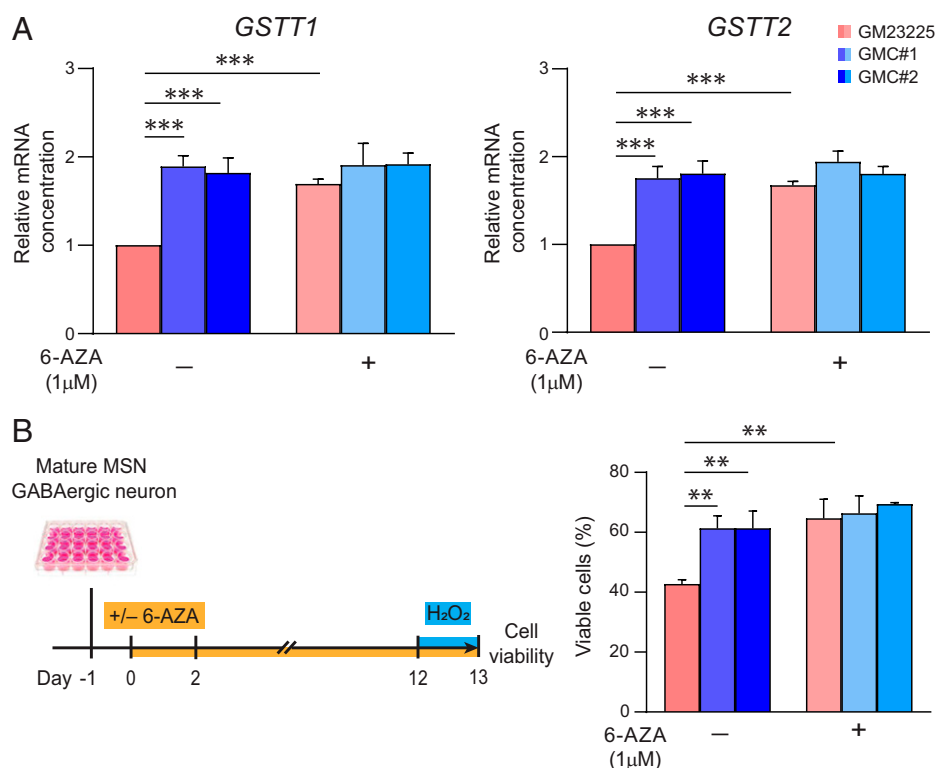


Fig. 4. 6-AZA-mediated modification of effects of mutant *HTT* on oxidative stress gene expression in MSN neurons. (A) *GSTT1* and *GSTT2* gene expression was analyzed by qRT-PCR with *SnRNA U6* as a loading control in GM23225-, GMC#1-, and GMC#2-differentiated MSN GABAergic neurons with or without 6-AZA treatment. The *GSTT1* and *GSTT2* mRNA levels relative to untreated GM23225 are shown. All the values shown are the mean \pm SD (B) Experimental outline for cell viability determination in MSN GABAergic neurons. Mature MSN GABAergic neurons derived from GM23225 (HD subject), or GMC#1 and GMC#2 (HD correction subject) were treated with 1 μ M 6-AZA for 13 d. 100 μ M H_2O_2 was added and cultures were incubated for an additional 24 h. Cell viability was determined by Trypsin blue assay. Values for samples not exposed to H_2O_2 or 6-AZA were set as 100%. ($n = 3$), $**P < 0.01$, $***P < 0.001$, in two-tailed paired Student's *t* test.

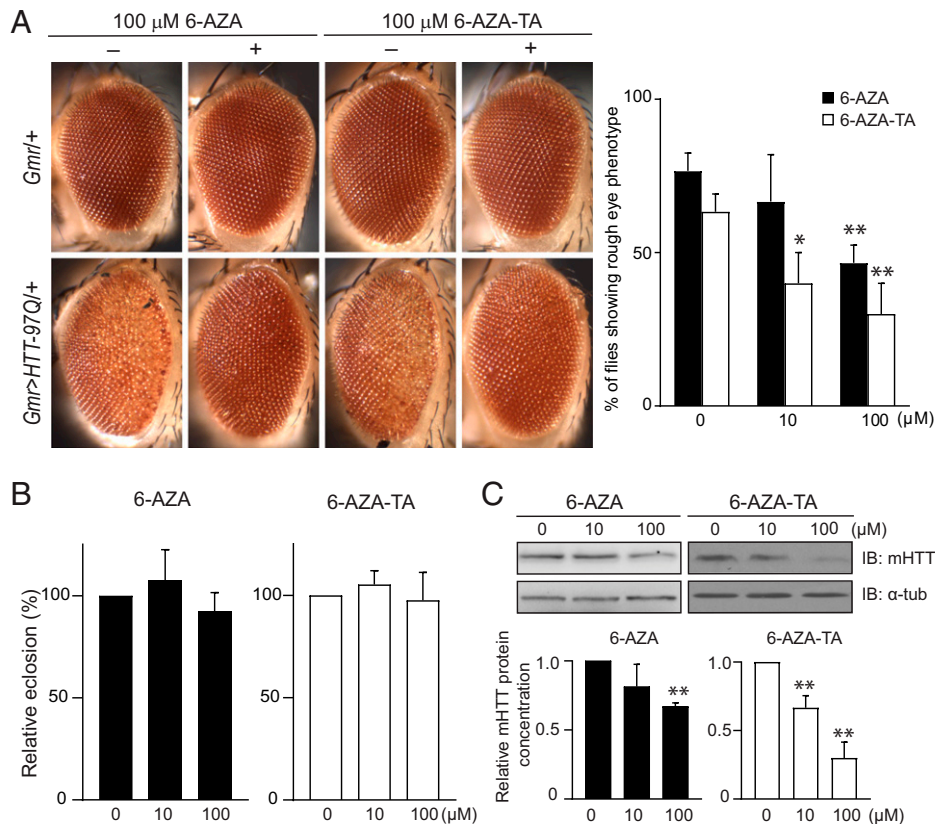


Fig. 5. Effect of 6-AZA and its prodrug on rough eye phenotype associated with expression of mutant HTT in *Drosophila*. (A) Representative images of compound eye of *Gmr* > *HTT-97Q*/⁺ flies developed from larvae cultured in agar containing 100 μ M of 6-AZA or its prodrug 6-AZA-TA (indicated as +). *Gmr*⁺ flies served as a control (top panel). Percentage of flies showing rough eye phenotype after culture of larvae in agar containing *Gmr* > *HTT-97Q*/⁺, 10 or 100 μ M 6-AZA or 6-AZA-TA. Ten flies were randomly picked from each experimental group and the number of flies showing the rough eye phenotype was determined by examination under a microscope. The values shown in this panel are the mean \pm SD for three independent experiments ($n = 10$, $N = 3$, $*P < 0.05$, $**P < 0.01$, two-tailed paired Student's *t* test). (B) 100 eggs of *w*¹¹¹⁸ strain were cultured in a vial containing 10 mL of media supplemented with 10 or 100 μ M of 6-AZA or 6-AZA-TA. Posteclosion flies were counted in each vial and the number of flies collected in untreated samples was set as 100%. ($n = 100$, $N = 3$, Error bars represent the SD, two-tailed paired Student's *t* test). (C) Mutant HTT protein was assessed by Western blotting using the same set of HD flies as described in A. α -tubulin was included as a loading control. The relative levels of mutant HTT in treated vs. untreated HD flies after normalization are shown. ($n = 3$; $**P < 0.01$, two-tailed paired Student's *t* test).

interference—which has been confirmed by two independent reporter assays and a direct biochemical assay—can lower the abundance of mutant *HTT* gene products in cultured cells and an HD animal model, and that chemical targeting of DSIF complex formation can mitigate phenotypic effects of repeat expansions. However, the broad and essential biochemical functions of DSIF (5, 8, 47), raise the prospect that therapeutic targeting of DSIF may be challenging. As SUPT4H and SUPT5H can act individually, as well as in complex with each other, the effects of targeting DSIF also may differ from the effects of targeting its individual components (48, 49).

Compounds of multiple chemical classes potentially may interfere with the SUPT4H-SUPT5H interaction. Among the compounds identified by our screening assays was 6-azauridine, a previously studied nucleoside inhibitor of de novo uridine-5'-monophosphate productive pathway (50) and consequently of nucleic acid synthesis (51) and cell division (52, 53). Addition of uridine to cell cultures reversed the effects of approximately equimolar amounts of 6-AZA on global nucleic acid synthesis without affecting mutant HTT expression, demonstrating the distinctness of these two effects of the compound.

Loss of medium spiny neurons (MSNs) in the striatum is a characteristic feature of HD and other neurodegenerative diseases (54, 55). We used CRISPR/Cas9 gene editing methodology to shorten the number of *HTT* gene CAG repeats in HD

patient MSNs to a nonpathological length (56), and found that shortening of repeats in these congenic cells was associated with diminished sensitivity to H₂O₂ exposure. Treatment with 6-AZA partially reversed the incremental sensitivity of cells containing expanded repeats, but did not affect H₂O₂ sensitivity in cells containing shorter repeats.

Analogous partial reversal of phenotypic effects of mutant HTT expression was observed also in the adult *Drosophila* compound eye, which has been widely used as a model for Huntington's Disease and other human neurodegenerative disorders (57). We did not detect any loss of *Drosophila* larval viability at a 6-AZA concentration that rescued animals displaying the rough eye phenotype. However, the ability of uridine supplementation to reverse the global effects of 6-AZA on nucleic acid synthesis in cell culture raises the possibility that such supplementation may prove useful also in mammalian models during *in vivo* studies.

Whereas the pathogenic effects of repeat expansions in HD and certain other diseases have been observed most clearly in neuronal cells (58), they are also evident in non-CNS tissues (59, 60). In our experiments, they were observed in MSNs, in neuronal cells, in blood cells, and in photoreceptor cells of the eye—and in replicating and nonreplicating cells. Whereas chemical interference with the SUPT4H-SUPT5H interaction has the potential for affecting multiple tissues simultaneously,

differences in the length of repeats as well as tissue-specific factors unrelated to DSIF may influence the results of such interference.

Materials and Methods

Plasmid Constructs. HA-SUPT4H and Flag-NGN fragments were amplified by PCR using pcDNA3-HA-SUPT4H and pcDNA3-Flag-NGN constructs. Substitution of the Zip protein encoding sequence of pcDNA3.1-Zip-GL1 and pcDNA3.1-Zip-GL2 (21) generated pcDNA3.1-SUPT4H-GL1 and pcDNA3.1-NGN-GL2, respectively. The HA-SUPT4H-GL1 and Flag-NGN-GL2 were then subcloned into pNEBR-X1-Hygro vector (New England Biolabs), under the control of RheoSwitch inducible promoter. Amino acid substitutions (M43I and M110I) were separately introduced into the GL1 and GL2 proteins to improve their stability (61). For concurrent expression of the SUPT4H-GL1 and NGN-GL2 proteins, a DNA fragment spanning the Flag-NGN-GL2 and containing a RheoSwitch-controlled promoter was cloned into pNEBR-X1-HA-SUPT4H-GL1. The plasmid carries a hygromycin resistant marker. A plasmid construct expressing intact Gluc was created by introducing a G418 resistant marker into pNEBR-X1-Gluc (New England Biolabs).

Stable Cell Lines. HEK293 cells were transfected with the pNEBR-R1 plasmid using lipofectamine 2000 (Invitrogen) and were selected by growth on media containing the antibiotic blasticidin at 10 $\mu\text{g}/\text{mL}$ A clone 293-R1, showing proficient RheoSwitch ligand 1 (RSL1)-dependent induction, was chosen for further construction. pNEBR-X1-HA-SUPT4H-GL1-Flag-NGN-GL2 was introduced into 293-R1. After selection on media containing hygromycin (250 $\mu\text{g}/\text{mL}$), a clone that exhibited a high level of SUPT4H-GL1 and NGN-GL2 expression upon the addition of RSL1 was selected and used for high-throughput screening. The clone was designated as M2-8. A stable clone G5, which expresses intact Gluc upon RSL1 induction, was also generated by transfecting pNEBR-X1-Gluc into 293-R1 cells.

Cell Culture. HEK293, 293-R1, M2-8, and G5 were cultured in Dulbecco's modified Eagle's medium (DMEM) with 10% FBS at 37 °C with 5% CO₂. The HD-lymphoblastoid cell line GM14044 was cultured in RPMI 1640 (Gibco) with 10% FBS at 37 °C with 5% CO₂. ST Hdh^{Q7/Q7} and ST Hdh^{Q111/Q111}, derived from striatal neurons of a knock-in Q7/Q7 or Q111/Q111 mouse, were cultured in DMEM (HyClone) supplemented with 15% FBS at 33 °C with 5% CO₂.

A human iPSC line GM23225, purchased from Coriell Institute (Camden NJ, USA), and two derived lines, GMC#1 and GMC#2, were grown on feeder layers of mitotically inactivated mouse embryonic fibroblasts and maintained in hESC medium, which is comprised of DMEM/F12 supplemented with 20% knockout serum replacement, 1% nonessential amino acids (NEAA), 2 mM L-glutamine, 100 μM 2-mercaptoethanol and 10 ng/mL basic fibroblast growth factor (bFGF).

Luciferase Assay. Cells were seeded in 96-well or 384-well white plates for 24 h of culture before adding RheoSwitch ligand 1 (RSL1) to induce luciferase gene expression. Compounds tested were added currently with RSL. After incubation for 24 h to allow for possible variation among compounds in rate of absorption or kinetics of interaction, and also allow for steady-state production of reporter gene proteins, culture media were removed by blotting onto thick paper towels. The plates were kept at -20 °C overnight before adding the lysis buffer (30 mM Tris-HCl, pH 8.0, 5 mM NaCl, 0.1% Triton X-100) containing 10 $\mu\text{g}/\text{mL}$ native coelenterazine (NanoLight Technology). The cells were lysed at room temperature for 1 h in the dark and the plates were shaken for ~1 min at the end of incubation. Luminescence signal intensities (integrated 100 ms) were measured using a Tecan Infinite M200 or Tecan Infinite M1000 luminometer.

High-Throughput Screening. High-throughput screening of compound libraries was conducted at the Stanford University High-Throughput Bioscience Center (HTBC). The libraries which were provided by HTBC consisted of ChemDiv (50K), SPECS (30K), Chembridge (23.5K), ChemDiv Kinase (10K), Library of Pharmacologically Active Compounds (LOPAC1280), NIH Clinical Collection (NIHCC) (446 compounds), NCI DTP (3084 compounds), Microsource Spectrum (2000 compounds), Biomol (now Enzo Life Sciences) ICCB Known Bioactives (480 compounds), and FDA Approved Drug Library (640 compounds). M2-8 or G5 cells were used in screens and were seeded in 384-well white plates at a density of 3000 cells/well. The compound concentration for screening was 10 μM .

The compounds 6-AZA and 6-AZA-TA were purchased from Sigma-Aldrich.

Co-Immunoprecipitation. M2-8 cells treated with RSL1 and 6-AZA for 24 h were collected and lysed in lysis buffer (30 mM Tris-HCl, pH 8.0, 5 mM NaCl, 0.1% Triton X-100). Cell lysates were incubated with Anti-Flag M2 magnetic beads (Sigma-Aldrich) at 4 °C for 3 h. After washing the beads three times with cold lysis buffer, precipitating proteins were analyzed by Western blot. ST Hdh^{Q111/Q111} cells treated with 10 μM 6-AZA in the absence or presence of uridine supplementation for 24 h were collected and lysed in RIPA buffer (50 mM Tris-HCl, pH 7.5, 150 mM NaCl, 1% Nonidet P-40, 1 mM Na₃VO₄, 1 mM DTT, 1 mM PMSF, and proteinase inhibitor mixture). Cell lysates were precleared with protein G beads (Roche) at 4 °C for 1 h and incubated with anti-SUPT4H antibody (Cell Signaling) in the presence of 10 μM 6-AZA at 4 °C overnight. After coincubation with protein G beads at 4 °C for 1 h, the beads were then washed three times with cold lysis buffer. The input and precipitating proteins were analyzed by Western blot.

Human HD-Lymphoblastoid Cell Line Treated with 6-AZA. The HD-lymphoblastoid cell line GM14044 containing 750 CAG repeats in the mutant HTT allele was purchased from Coriell Institute (Camden NJ, USA). The cells were seeded in a 6-well plate at a density of 3 \times 10⁵ cells/well and incubated with 6-AZA for 72 h. By the end of treatment, cells were collected and subjected to Western blot analysis.

Mouse Striatal Neuron Cell Lines Treated with 6-AZA. The mouse striatal neuron cell lines, ST Hdh^{Q7/Q7} and ST Hdh^{Q111/Q111}, were incubated with various concentrations of 6-AZA for 12 h, and total RNA was collected for analysis of gene expression. Analogously, cells treated with 6-AZA for 24 h were collected for Western blot analysis. To assess cell viability, adherent cells were collected from plates at the end of treatment and the number of viable cells were counted using hemocytometer after Trypan blue staining. In uridine supplementation experiments, ST Hdh^{Q111/Q111} cells were seeded at a density of 8 \times 10⁵ cells/well in 6-well plates and treated with 6-AZA (10 μM) plus indicated concentrations of uridine (Sigma) for 24 h. The cells were subjected to assess the number of viable cells by Trypan blue exclusion assay and determine the expression of mutant HTT by Western blot assay.

Western Blot Analysis. Cells were lysed with RIPA buffer [50 mM Tris-HCl, pH 7.5, 150 mM NaCl, 1% Nonidet P-40, 0.1% sodium dodecyl sulfate (SDS), and 1% sodium deoxycholate supplemented with 1mM Na₃VO₄], 1 mM DTT, 1 mM PMSF, and a protease inhibitor mixture (Sigma). For GABAergic neuron samples, SDS was increased to 0.5% in RIPA buffer to enhance lysate solubility. Equal amounts of protein lysates were resolved through 3-8% gradient Tris-acetate gel electrophoresis (Invitrogen) or 12% SDS-PAGE, transferred onto nitrocellulose membranes (GE), and probed with primary antibodies for 1 h. After incubation with horseradish peroxidase-conjugated secondary antibodies, the immunoreactive signals were detected by an enhanced chemiluminescence (ECL) reagent (PerkinElmer), recorded by ImageQuant LAS 4000 mini, and quantitatively analyzed using Multi Gauge Software. Gradient Tris-acetate gel electrophoresis was employed to analyze HTT and SUPT5H. SDS-PAGE was used for analysis of SUPT4H, TBP, and α -tubulin. Nitrocellulose membranes also were stained with LI-COR REVERT Kit (LI-COR) for total protein detection. Membranes were scanned by Odyssey imaging system and quantified using Li-Cor Odyssey software.

For *Drosophila* samples, 15 male and 15 female *Drosophila* were frozen at -80 °C. After decapitation, the heads were collected and homogenized in 1 \times sample buffer. Equal amounts of protein lysates were separated by 10% SDS-PAGE, transferred onto nitrocellulose membranes, and probed with anti-HTT (1:5,000) or anti- α -tubulin antibody (1:10000) for 1 h. After incubation with horseradish peroxidase-conjugated secondary antibodies for another 1 h, immunoreactive signals were detected using the ECL reagent (PerkinElmer).

Antibodies. Anti-Gluc (E8023, New England Biolabs), Anti-HA-Peroxidase High Affinity (3F10, Roche), Anti-Flag M5 (F4042, Sigma), Anti- α -tubulin (DM1A, Sigma; AJ1034a, ABGENT), Anti-poly Glutamine (MAB1574, Millipore), Anti-HTT (MAB2166, Millipore), Anti-SUPT4H (D3P2W, Cell Signaling), Anti-SUPT5H (611107, BD Biosciences), Anti-TBP (58C9, Sigma), and Anti-GFP (GTX113617, GeneTex) antibodies were purchased. For detection of human mutant HTT in HD-*Drosophila*, anti-HTT antibody was generously provided by Dr. Yijiang Chem.

Neural Differentiation of HD-iPSC. Induced differentiation of GABAergic neurons was performed as described previously (38). First, iPSCs were dissociated by 1× dispase (1 mg/mL), diluted by MEF growth medium (DMEM supplemented with 10% FBS, 1% NEAA, 2 mM L-glutamine), and seeded in ultra-low attachment dishes (Corning). Cells were incubated in hESC medium containing 100 nM LDN193189 and 10 μ M SB431542, but without basic fibroblast growth factor (bFGF) for 3 d, followed by culturing in N2 medium (DMEM/F12, 1 \times N2 supplement, 1% NEAA, 2 mM L-glutamine, 1 mM sodium pyruvate, 20 ng/mL bFGF, 100 nM LDN 193189, and 10 μ M SB 431542) for another 2 d. Embryonic bodies (EBs) were then collected and placed on 6-cm dishes with MEF medium. 24 h post seeding, the growth medium was changed from MEF to N2 medium and replenished every other day for 2–3 consecutive weeks to produce neural progenitor cells (NPCs). For induced differentiation of GABAergic neurons from NPC, cells with rosette-like structures were picked by needles, transferred to Matrigel-coated dishes, and cultured for 3–4 wk in N2/B27 medium (mixture of DMEM/F12 and Neurobasal medium (1:1) supplemented with 0.5 \times N2, 0.5 \times B27, 1% NEAA, 0.5 mM sodium pyruvate, 2 mM L-glutamine, and 10 ng/mL bFGF). During this period, neurospheres were isolated/purified from cell population on a weekly basis. Mature GABAergic neurons were isolated and grown in B27 medium (Neurobasal medium supplemented with 1 \times B27 supplement, 1% NEAA, and 2 mM L-glutamine) for 4–6 wk, with the medium being changed every 3 d. Differentiation of MSN GABAergic neurons was characterized by immunocytochemistry.

HD GABAergic Neurons Treated with 6-AZA. Neural differentiation of HD-iPSCs as described above at the 11th week were pretreated with 10 μ M Y27632 (Merck) overnight. Cells were dissociated into single cells by TrypLE and neutralized by MEF medium containing 10 μ M Y27632. After washing with B27 medium containing 10 μ M Y27632, cells were seeded on Matrigel-coated plates and incubated in the same medium overnight. The GABAergic neurons were then treated with different doses of 6-AZA in B27 medium for 13 d, with medium being changed every other day.

Viability of GABAergic Neurons Under H₂O₂ Exposure. MSN GABAergic neurons differentiated from either GM23225 (stem cells from HD patient), or GMC#1 and GMC#2, were treated with/without 1 μ M of 6-AZA for 13 d as described above. 100 μ M H₂O₂ were added into medium 24 h prior to the collection of cells. Cells were subjected to Trypan blue exclusion assay to measure the number of viable cells using hemocytometer.

Fly Stocks. The lines of *Gmr-gal4*, *UAS-mCD8-GFP*, and *w¹¹¹⁸* were acquired from Bloomington Stock Center. *UAS-HTT-97Q* was obtained from Dr. L. Marsh (University of California, Irvine, CA, USA) (62). Recombinant fly lines (*Gmr-gal4* > *HTT-97Q* and *Gmr-gal4* > *mCD8-GFP*) expressing human HTT exon1 containing 97 repeats of CAG or mCD8-GFP under the control of *Gmr-gal4* were generated through conventional genetic crosses. All fly stocks were maintained at 25 °C on a standard cornmeal yeast agar medium.

Compound Efficacy Test in HD-Fly. 15 male homozygous *Gmr-gal4* > *HTT-97Q* flies were crossed with 15 virgin *w¹¹¹⁸* female flies in a vial containing 10 mL of media supplemented with chemical compounds at a final concentration of 10 or 100 μ M. Parental flies were removed from vial in a week. 4-d-old heterozygous progenies were then collected for assessment of rough eye phenotypes and Western blot analysis. As control, 15 male and female homozygous *Gmr-gal4* > *mCD8-GFP* flies were crossed and followed the same experimental procedure as described above to assess GFP expression. Images of compound

eyes were captured using a camera (CoolSNAP 5.0, Photometrics) mounted onto a Leica DMR upright microscope. Imaging software Helicon Focus (HeliconSoft) was used to increase the depth of field and create a composite image. 10 flies were analyzed in each treatment group and compared to that of untreated control group. *Gmr-gal4* flies also were included as a control. Each experiment was performed independently at least three times.

Compound Toxicity Test in *Drosophila*. 100 eggs laid by the *w¹¹¹⁸* strain were collected and cultured in a vial containing 10 mL of media supplemented with test compound at a final concentration of 10 or 100 μ M. The vials were incubated at 25 °C for 10 d. Post-eclosion flies were counted and compared to the number of flies in a control vial, which contains only growth media. Each experiment was conducted independently at least three times.

Statistical Analysis. Unless stated otherwise, the results shown are representative of replicated experiments and the values presented are the means \pm SDs from triplicate samples. Statistical analyses were carried out using two-tailed Student's *t* test to compare the mean values of two groups. *P* < 0.05 was considered statistically significant.

Data Availability. All data related to the current study are present in the paper or *SI Appendix*. All materials created in this study are available with material transfer agreements approved by Stanford University and National Yang Ming Chiao Tung University to any researcher for purposes of reproducing or extending the analysis.

ACKNOWLEDGMENTS. We thank Dr. Chao-Wen Wang for providing pRS413-GDP-VN-C and pRS413-GDP-VC-C plasmid constructs, Dr. Stephen W. Michnick for providing *Gaussia* luciferase constructs, and Dr. Yijuan Chern for custom-made anti-HTT antibody. We thank Bruce Koch, Daria Mochley-Rosen, Kevin Grimes, Steven Schow and Mark Smith for advice. These studies were supported by grants from the U.S. National Institutes of Health (1R01NS08581201 to S.N.C.), the SPARK Translational Medicine Program of Stanford University, and the Harrington Discovery Institute to S.N.C., and by grants from Academia Sinica, the Ministry of Science and Technology (MOST103-2325-B-010-004, MOST104-2320-B-010-021-MY3, MOST107-2320-B-010-036-MY3, MOST110-2327-B-A49A-503, AS-103-TP-B10, AS-106-TP-L13-3 to T.H.C.). The project was also supported by the Brain Research Center, National Yang Ming Chiao Tung University, by the Featured Areas Research Center Program within the framework of the Higher Education Sprout Project by the Ministry of Education (MOE) in Taiwan, and by funds from the K.-T. Li professorship held by S.N.C. at Stanford University. Stanford University and National Yang Ming Chiao Tung University have received patents for reduction of the deleterious activity of extended nucleotide repeat-containing genes.

Author affiliations: ^aDepartment of Genetics, Stanford University School of Medicine, Stanford, CA 94305; ^bTaiwan International Graduate Program in Molecular Medicine, National Yang Ming Chiao Tung University and Academia Sinica, Taipei, 11529, Taiwan; ^cInstitute of Biochemistry and Molecular Biology, National Yang Ming Chiao Tung University, Taipei, 11221, Taiwan; ^dInstitute of Biotechnology and Pharmaceutical Research, National Health Research Institutes, Zhunan, 35053, Taiwan; ^eDepartment of Life Science and Institute of Genome Sciences, National Yang Ming Chiao Tung University, Taipei, 11221, Taiwan; ^fInstitute of Biomedical Informatics, National Yang Ming Chiao Tung University, Taipei, 11221, Taiwan; ^gDepartment of Life Science, National Taiwan Normal University, Taipei, 11677, Taiwan; ^hInstitute of Cellular and Organismic Biology, Academia Sinica, Taipei, 11529, Taiwan; and ⁱBrain Research Center, National Yang Ming Chiao Tung University, Taipei, 11221, Taiwan

- H. Paulson, Repeat expansion diseases. *Handb. Clin. Neurol.* **147**, 105–123 (2018).
- C. M. Rodriguez, P. K. Todd, New pathologic mechanisms in nucleotide repeat expansion disorders. *Neurobiol. Dis.* **130**, 104515 (2019).
- I. Malik, C. P. Kelley, E. T. Wang, P. K. Todd, Molecular mechanisms underlying nucleotide repeat expansion disorders. *Nat. Rev. Mol. Cell Biol.* (2021).
- T. Wada *et al.*, DSIF, a novel transcription elongation factor that regulates RNA polymerase II processivity, is composed of human Spt4 and Spt5 homologs. *Genes Dev.* **12**, 343–356 (1998).
- Y. Yamaguchi *et al.*, Structure and function of the human transcription elongation factor DSIF. *J. Biol. Chem.* **274**, 8085–8092 (1999).
- P. B. Mason, K. Struhl, Distinction and relationship between elongation rate and processivity of RNA polymerase II in vivo. *Mol. Cell* **17**, 831–840 (2005).
- F. W. Martinez-Rucobo, S. Sainsbury, A. C. Cheung, P. Cramer, Architecture of the RNA polymerase-Spt4/5 complex and basis of universal transcription processivity. *EMBO J.* **30**, 1302–1310 (2011).
- T. M. Decker, Mechanisms of transcription elongation factor DSIF (Spt4-Spt5). *J. Mol. Biol.* **433**, 166657 (2021).
- C. R. Liu *et al.*, Spt4 is selectively required for transcription of extended trinucleotide repeats. *Cell* **148**, 690–701 (2012).
- H. M. Cheng *et al.*, Effects on murine behavior and lifespan of selectively decreasing expression of mutant huntingtin allele by *supt4h* knockdown. *PLoS Genet.* **11**, e1005043 (2015).
- N. J. Kramer *et al.*, Spt4 selectively regulates the expression of C9orf72 sense and antisense mutant transcripts. *Science* **353**, 708–712 (2016).
- N. Furuta, S. Tsukagoshi, K. Hirayanagi, Y. Ikeda, Suppression of the yeast elongation factor Spt4 ortholog reduces expanded SCA36 GGCCUG repeat aggregation and cytotoxicity. *Brain Res.* **1711**, 29–40 (2019).
- A. Bahat, O. Lahav, A. Plotnikov, D. Leshkowitz, R. Dikstein, Targeting Spt5-Pol II by Small-Molecule Inhibitors Uncouples Distinct Activities and Reveals Additional Regulatory Roles. *Mol. Cell* **76**, 617–631.e4 (2019).

14. H. J. Park *et al.*, SUPT4H1-edited stem cell therapy rescues neuronal dysfunction in a mouse model for Huntington's disease. *NPJ Regen. Med.* **7**, 8 (2022).
15. N. S. Caron, G. E. B. Wright, M. R. Hayden, Huntington Disease. in *GeneReview* (National Center for Biotechnology Information, Online) (2020).
16. P. Dayalu, R. L. Albin, Huntington disease: Pathogenesis and treatment. *Neurol. Clin.* **33**, 101-114 (2015).
17. A. Kumar *et al.*, Huntington's disease: An update of therapeutic strategies. *Gene* **556**, 91-97 (2015).
18. J. Smeyers, E. G. Banchi, M. Latouche, C9ORF72: What it is, What it does, and why it matters. *Front. Cell. Neurosci.* **15**, 661447 (2021).
19. H. Kobayashi *et al.*, Expansion of intronic GGCCGT hexanucleotide repeat in NOPS6 causes SCA36, a type of spinocerebellar ataxia accompanied by motor neuron involvement. *Am. J. Hum. Genet.* **89**, 121-130 (2011).
20. S. Mizielińska, A. M. Isaacs, NEURODEGENERATION. One target for amyotrophic lateral sclerosis therapy? *Science* **353**, 647-648 (2016).
21. I. Remy, S. W. Michnick, A highly sensitive protein-protein interaction assay based on Gaussia luciferase. *Nat. Methods* **3**, 977-979 (2006).
22. T. K. Kerppola, Design and implementation of bimolecular fluorescence complementation (BiFC) assays for the visualization of protein interactions in living cells. *Nat. Protoc.* **1**, 1278-1286 (2006).
23. J. J. Jaffe, R. E. Handschumacher, A. D. Welch, Studies on the carcinostatic activity in mice of 6-azauracil riboside (azauridine), in comparison with that of 6-azauracil. *Yale J. Biol. Med.* **30**, 168-175 (1957).
24. G. A. Hartzog, T. Wada, H. Handa, F. Winston, Evidence that Spt4, Spt5, and Spt6 control transcription elongation by RNA polymerase II in *Saccharomyces cerevisiae*. *Genes Dev.* **12**, 357-369 (1998).
25. R. Malbec *et al.*, μ LAS: Sizing of expanded trinucleotide repeats with femtomolar sensitivity in less than 5 minutes. *Sci. Rep.* **9**, 23 (2019).
26. G. A. Ruiz Buendía *et al.*, Three-dimensional chromatin interactions remain stable upon CAG/CTG repeat expansion. *Sci. Adv.* **6**, eaaz4012 (2020).
27. M. A. Nance, V. Mathias-Hagen, G. Breningstall, M. J. Wick, R. C. McGlennen, Analysis of a very large trinucleotide repeat in a patient with juvenile Huntington's disease. *Neurology* **52**, 392-394 (1999).
28. F. Trettel *et al.*, Dominant phenotypes produced by the HD mutation in STHdh(Q111) striatal cells. *Hum. Mol. Genet.* **9**, 2799-2809 (2000).
29. A. Parent, Extrinsic connections of the basal ganglia. *Trends Neurosci.* **13**, 254-258 (1990).
30. K. Griesi-Oliveira *et al.*, Transcriptome of iPSC-derived neuronal cells reveals a module of co-expressed genes consistently associated with autism spectrum disorder. *Mol. Psychiatry* (2020).
31. I. H. Park *et al.*, Disease-specific induced pluripotent stem cells. *Cell* **134**, 877-886 (2008).
32. R. Alhayaza, E. Haque, C. Karbasiafshar, F. W. Sellke, M. R. Abid, The Relationship Between Reactive Oxygen Species and Endothelial Cell Metabolism. *Front Chem.* **8**, 592688 (2020).
33. J. D. Hayes, J. U. Flanagan, I. R. Jowsey, Glutathione transferases. *Annu. Rev. Pharmacol. Toxicol.* **45**, 51-88 (2005).
34. E. Laborde, Glutathione transferases as mediators of signaling pathways involved in cell proliferation and cell death. *Cell Death Differ.* **17**, 1373-1380 (2010).
35. A. U. Joshi, D. Mochly-Rosen, Mortal engines: Mitochondrial bioenergetics and dysfunction in neurodegenerative diseases. *Pharmacol. Res.* **138**, 2-15 (2018).
36. Y. Wu, M. Chen, J. Jiang, Mitochondrial dysfunction in neurodegenerative diseases and drug targets via apoptotic signaling. *Mitochondrion* **49**, 35-45 (2019).
37. M. Focchetti *et al.*, Neuroglobin and mitochondria: The impact on neurodegenerative diseases. *Arch. Biochem. Biophys.* **701**, 108823 (2021).
38. F. L. Chiu *et al.*, Elucidating the role of the A2A adenosine receptor in neurodegeneration using neurons derived from Huntington's disease iPSCs. *Hum. Mol. Genet.* **24**, 6066-6079 (2015).
39. N. Allocati, M. Masulli, C. Di Ilio, L. Federici, Glutathione transferases: Substrates, inhibitors and pro-drugs in cancer and neurodegenerative diseases. *Oncogenesis* **7**, 8 (2018).
40. L. Quinti *et al.*, SIRT2- and NRF2-Targeting Thiazole-Containing Compound with Therapeutic Activity in Huntington's Disease Models. *Cell Chem. Biol.* **23**, 849-861 (2016).
41. M. Ribeiro, A. C. Silva, J. Rodrigues, L. Naia, A. C. Rego, Oxidizing effects of exogenous stressors in Huntington's disease knock-in striatal cells-protective effect of cystamine and creatine. *Toxicol. Sci.* **136**, 487-499 (2013).
42. S. Dasari *et al.*, Genetic polymorphism of glutathione S-transferases: Relevance to neurological disorders. *Pathophysiology* **25**, 285-292 (2018).
43. G. P. Bates, E. Hockly, Experimental therapeutics in Huntington's disease: Are models useful for therapeutic trials? *Curr. Opin. Neurol.* **16**, 465-470 (2003).
44. B. Mugat, M. L. Parmentier, N. Bonneaud, H. Y. Chan, F. Maschat, Protective role of Engrailed in a *Drosophila* model of Huntington's disease. *Hum. Mol. Genet.* **17**, 3601-3616 (2008).
45. W. C. Lee, M. Yoshihara, J. T. Littleton, Cytoplasmic aggregates trap polyglutamine-containing proteins and block axonal transport in a *Drosophila* model of Huntington's disease. *Proc. Natl. Acad. Sci. U.S.A.* **101**, 3224-3229 (2004).
46. E. A. Lewis, G. A. Smith, Using *Drosophila* models of Huntington's disease as a translatable tool. *J. Neurosci. Methods* **265**, 89-98 (2016).
47. G. A. Hartzog, J. Fu, The Spt4-Spt5 complex: A multi-faceted regulator of transcription elongation. *Biochim. Biophys. Acta* **1829**, 105-115 (2013).
48. G. Diamant, A. Bahat, R. Dikstein, The elongation factor Spt5 facilitates transcription initiation for rapid induction of inflammatory-response genes. *Nat. Commun.* **7**, 11547 (2016).
49. J. Fitz, T. Neumann, R. Pavri, Regulation of RNA polymerase II processivity by Spt5 is restricted to narrow window during elongation. *EMBO J.* **37**, e97965 (2018).
50. N. Wu, Y. Mo, J. Gao, E. F. Pai, Electrostatic stress in catalysis: Structure and mechanism of the enzyme orotidine monophosphate decarboxylase. *Proc. Natl. Acad. Sci. U.S.A.* **97**, 2017-2022 (2000).
51. A. Cihák, J. Vesely, J. Skoda, Azapyrimidine nucleosides: Metabolism and inhibitory mechanisms. *Adv. Enzyme Regul.* **24**, 335-354 (1985).
52. L. L. Wotring, L. B. Townsend, Identification of 6-azauridine triphosphate in L1210 cells and its possible relevance to cytotoxicity. *Cancer Res.* **49**, 289-294 (1989).
53. G. W. Schaeffer, T. Sorokin, Growth inhibition of tobacco tissue cultures with 6-azauracil, 6-azauridine and maleic hydrazide. *Plant Physiol.* **41**, 971-975 (1966).
54. P. Zheng, J. Kozloski, Striatal network models of Huntington's disease dysfunction phenotypes. *Front. Comput. Neurosci.* **11**, 70 (2017).
55. D. Bano, F. Zanetti, Y. Mende, P. Nicotera, Neurodegenerative processes in Huntington's disease. *Cell Death Dis.* **2**, e228 (2011).
56. X. Xu *et al.*, Reversal of phenotypic abnormalities by CRISPR/Cas9-mediated gene correction in Huntington disease patient-derived induced pluripotent stem cells. *Stem Cell Reports* **8**, 619-633 (2017).
57. L. McGurk, A. Berson, N. M. Bonini, *Drosophila* as an in vivo model for human neurodegenerative disease. *Genetics* **201**, 377-402 (2015).
58. M. Gray, Astrocytes in Huntington's disease. *Adv. Exp. Med. Biol.* **1175**, 355-381 (2019).
59. J. B. Carroll, G. P. Bates, J. Steffan, C. Saft, S. J. Tabrizi, Treating the whole body in Huntington's disease. *Lancet Neurol.* **14**, 1135-1142 (2015).
60. E. Wild *et al.*, Abnormal peripheral chemokine profile in Huntington's disease. *PLoS Curr.* **3**, RRN1231 (2011).
61. J. D. Hulleman, S. J. Brown, H. Rosen, J. W. Kelly, A high-throughput cell-based Gaussia luciferase reporter assay for identifying modulators of fibulin-3 secretion. *J. Biomol. Screen.* **18**, 647-658 (2013).
62. J. S. Steffan *et al.*, SUMO modification of Huntingtin and Huntington's disease pathology. *Science* **304**, 100-104 (2004).